

Supporting Information

pH-Gated Bidirectional Nanoassembly Switches: Self-Ratiometric D-Penicillamine Sensing via AIE- Active Au(I)-TCEP-Cd(II) Coordination Dynamics

Kunyang Li, †^{ab} Yelan Xiao, †^{ab} Yafang Sun, ^{ab} Zhi He, ^{ab} Jiarong Tian, ^{ab} Lei Su, ^{ab} Xueji Zhang ^{ab} and Tong Shu*^{ab}

^a Shenzhen Key Laboratory for Nano-Biosensing Technology, School of Biomedical Engineering, Shenzhen University Medical School, Shenzhen University, Shenzhen 518060, China

^b Marshall Laboratory of Biomedical Engineering, Shenzhen University Medical School, Shenzhen University, Shenzhen 518060, China

‡Kunyang Li and Yelan Xiao contributed equally to this work.

**Correspondence to:*

Tong Shu

shutong@szu.edu.cn

Table of Contents

1. Supporting Figures	S3
Figures S1-S20	S3
2. Supporting Table	S22
Table S1-S2	S22

1. Supporting Figures

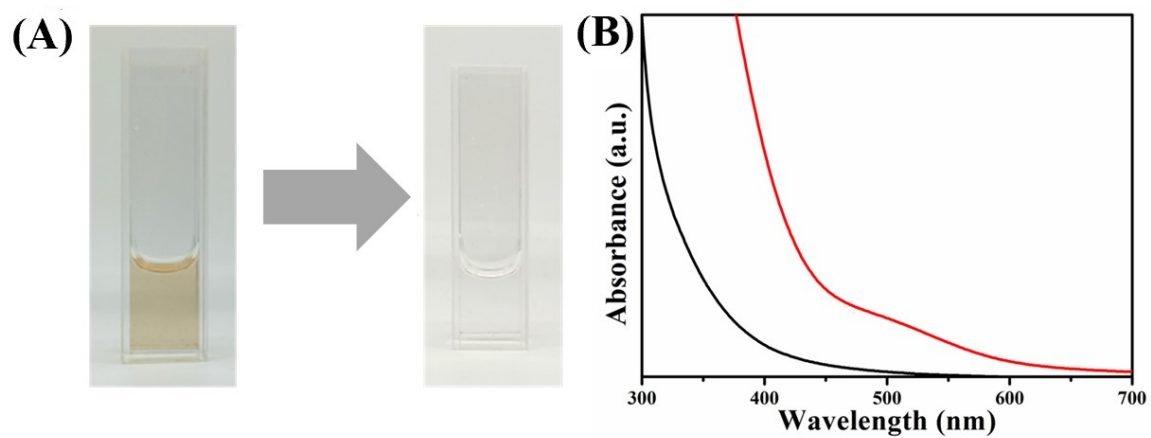


Fig. S1 (A) Photos of AuNCs@BSA solution before (left) and after (right) reacting with TCEP at pH 8. (B) UV-vis absorption spectra AuNCs@BSA solution before (red line) and after (black line) reacting with TCEP.

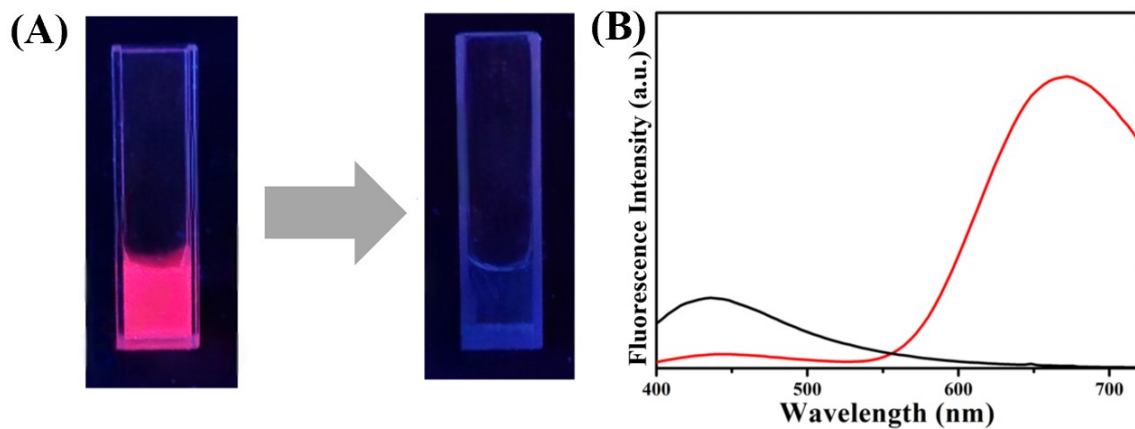


Fig. S2 (A) Photos of AuNCs@BSA solution before (left) and after (right) reacting with TCEP at pH 8 under UV light. (B) Luminescent spectra of AuNCs@BSA solution before (red line) and after (black line) reacting with TCEP.

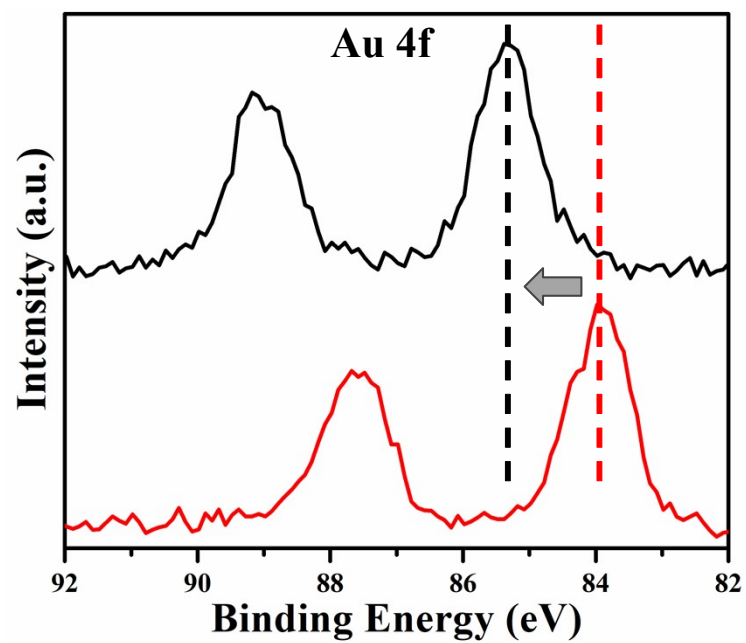


Fig. S3 XPS spectra of Au4f for the AuNCs@BSA before (red line) and after (black line) reacting with TCEP.

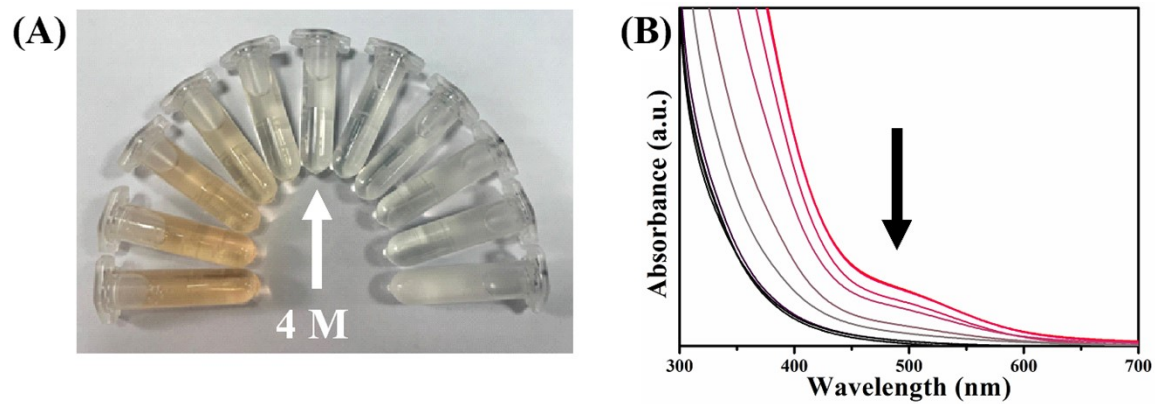


Fig. S4 Photo of samples under visible light (A) and the corresponding UV-vis absorption spectra (B) for different TCEP doses of AuNCs@BSA (the change in color from the red line to the black line indicates that the dose of TCEP is constantly increasing).

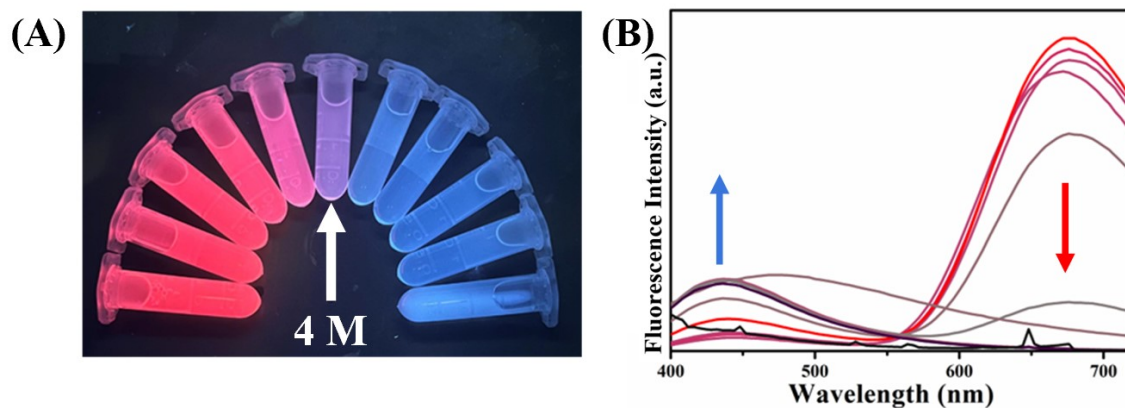


Fig. S5 Photo in the UV box (A) (TCEP content added from left to right, the content is 0, 0.5, 1, 2, 3, 4, 6, 8, 9, 18, 30 M) and fluorescence emission spectra (B) for different TCEP doses of AuNCs@BSA (the change in color from the red line to the black line indicates that the dose of TCEP is constantly increasing).

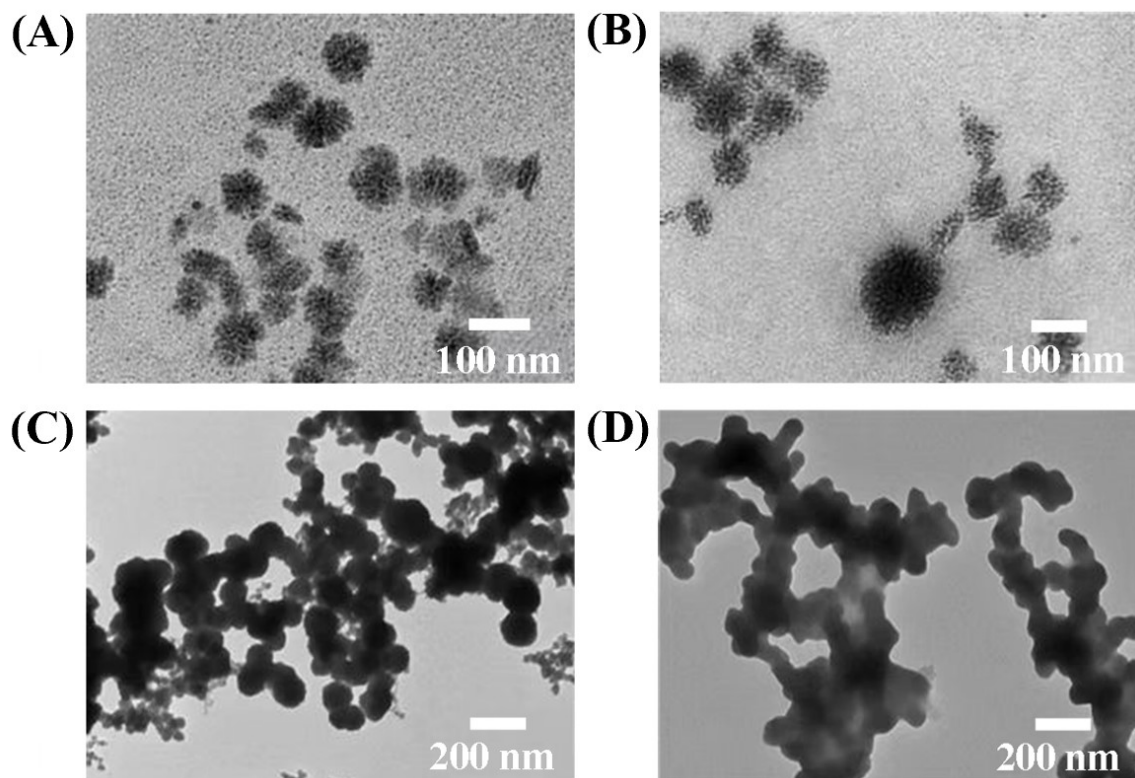


Fig. S6 TEM images of different concentration of Cd^{2+} : (A) 10 mM, (B) 16 mM, (C) 30 mM, (D) 60 mM.

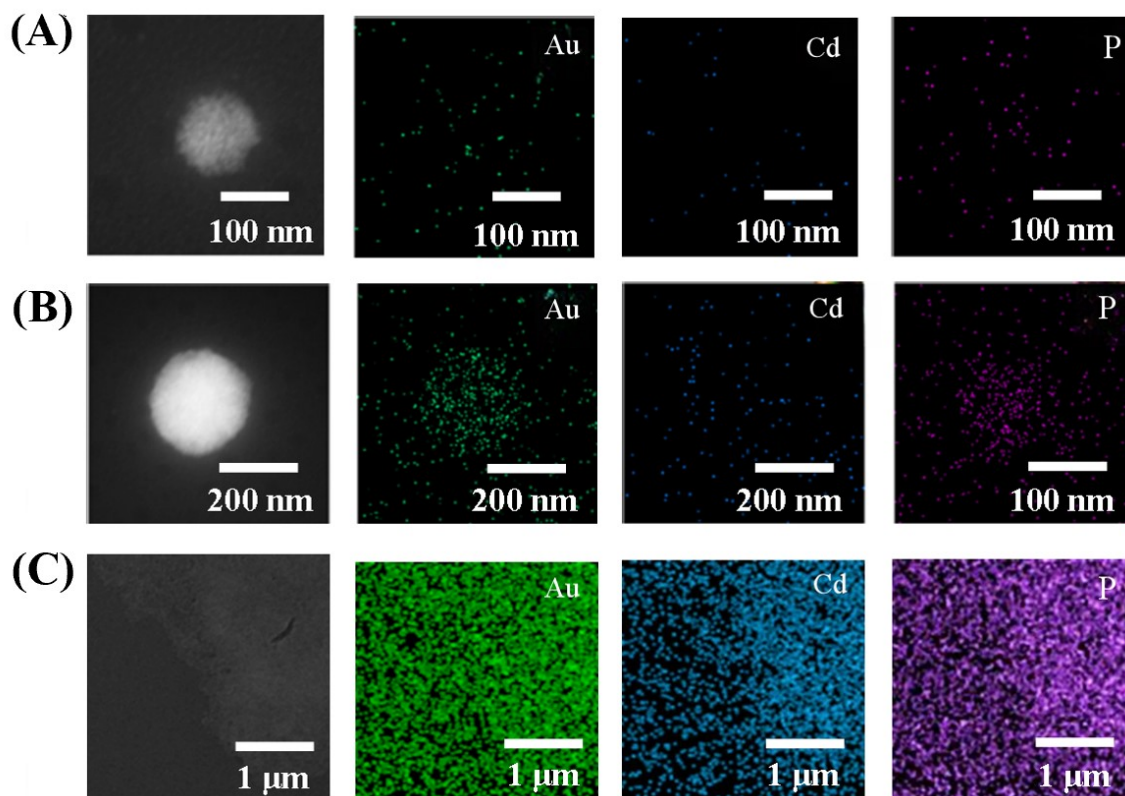


Fig. S7 Distribution of Au, Cd, and P elements in different materials: (A) 100 nm snowflake like material. (B) 120 nm circular material. (C) supramolecular aggregation material.

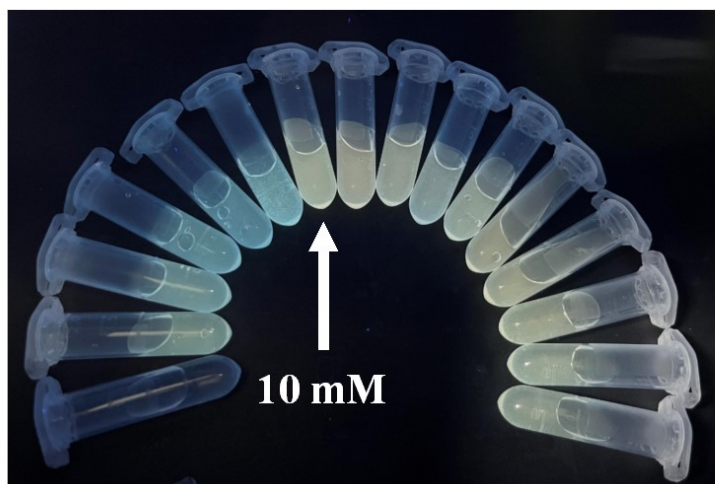


Fig. S8 Photos of Au(I)-TCEP with different Cd²⁺ concentrations in UV box (from left to right, the content is 0, 1, 3, 4, 6, 8, 10, 12, 14, 16, 20, 24, 30, 40, 50, 60 mM).

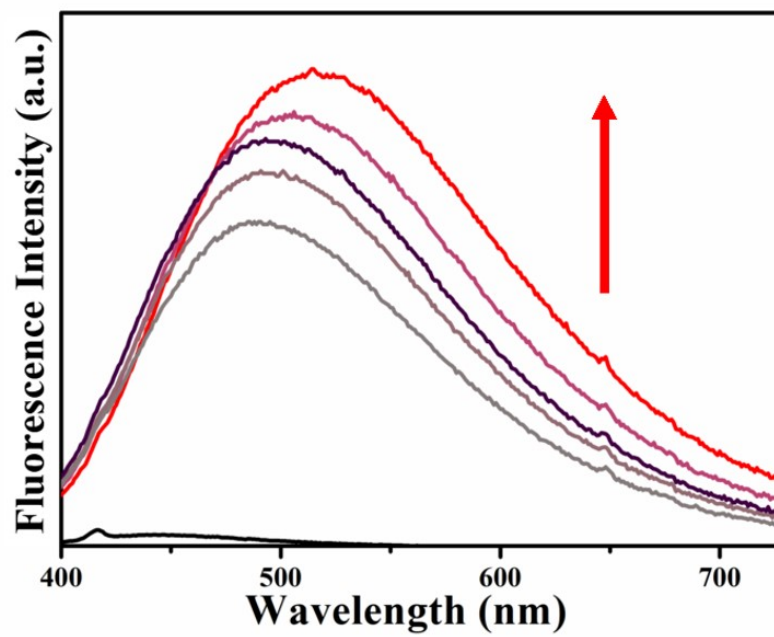


Fig. S9 Fluorescence emission spectra of Au(I)-TCEP solutions with the Cd²⁺ concentration of 0, 1, 3, 4, 6, 8 mM.

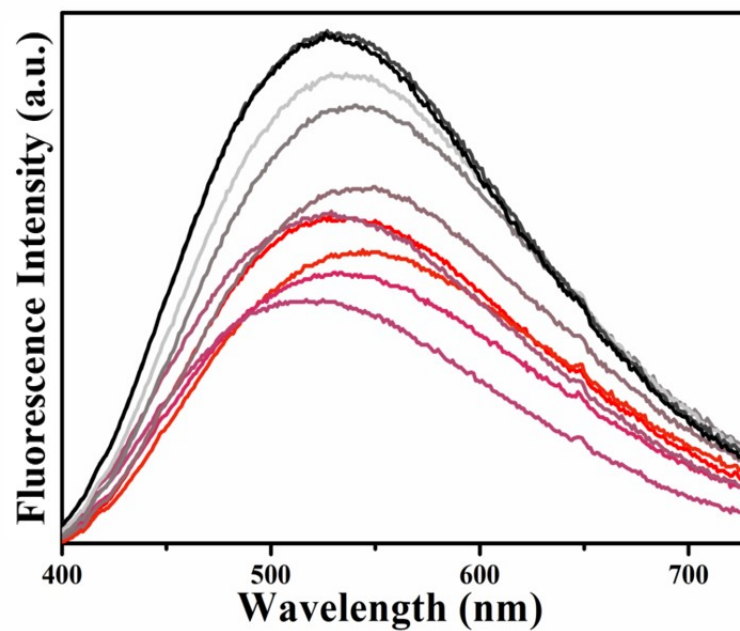


Fig. S10 Fluorescence emission spectra of Au(I)-TCEP with the Cd²⁺ concentrations in the range of 10-60 mM.

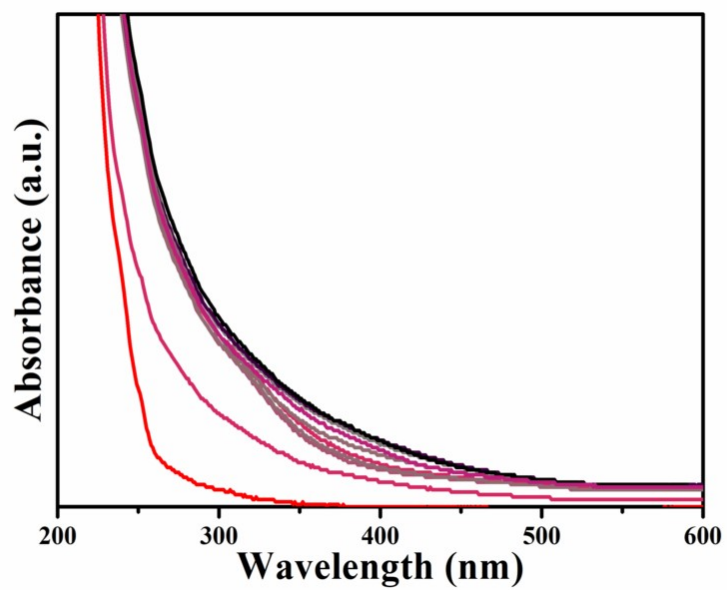


Fig. S11 UV absorption spectra of Au(I)-TCEP with different Cd²⁺ concentrations (red to black lines indicate a gradual increase in Cd concentrations).

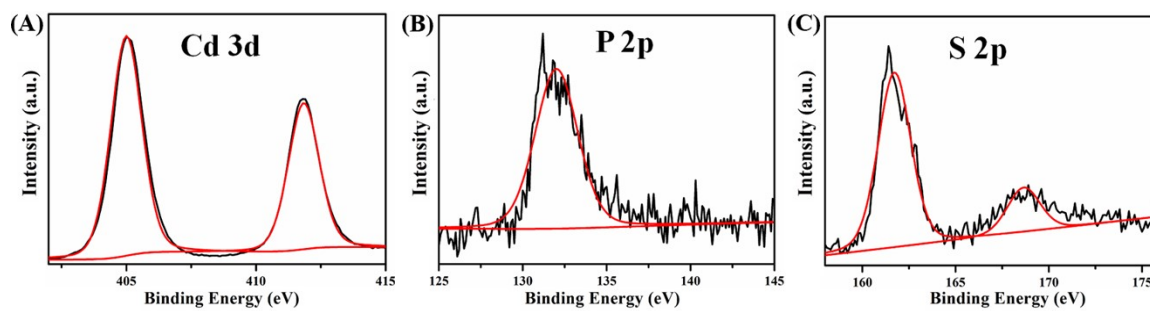


Fig. S12 XPS spectra of different elements in Au(I)-TCEP-Cd(II): (A) Cd, (B) P, (C)

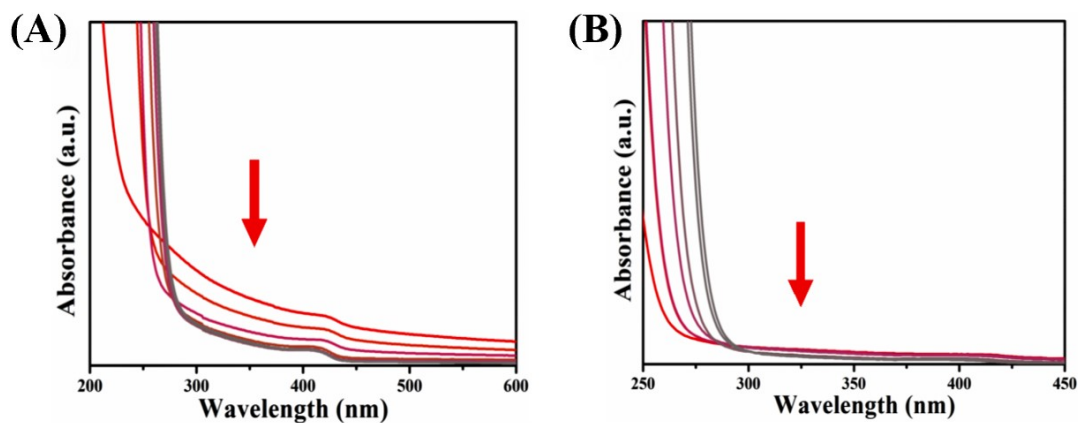


Fig. S13 (A) UV absorbance changes of Au(I)-TCEP-Cd(II) nanoaggregates with increasing DPA concentration at pH 7 (from red to black indicating a gradual increase in DPA concentration). (B) UV absorbance changes pf Au(I)-TCEP-Cd(II) nanoaggregates with increasing DPA concentration at pH 9 (from red to black indicating a gradual increase in DPA concentration).

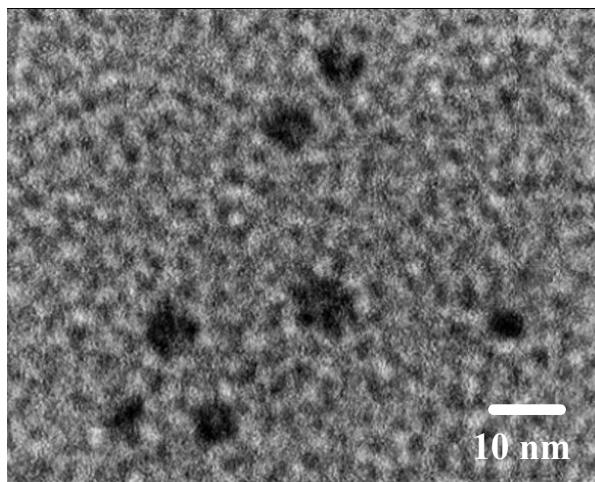


Fig. S14 TEM image of Au(I)-TCEP-Cd(II) after adding DPA (pH 7).

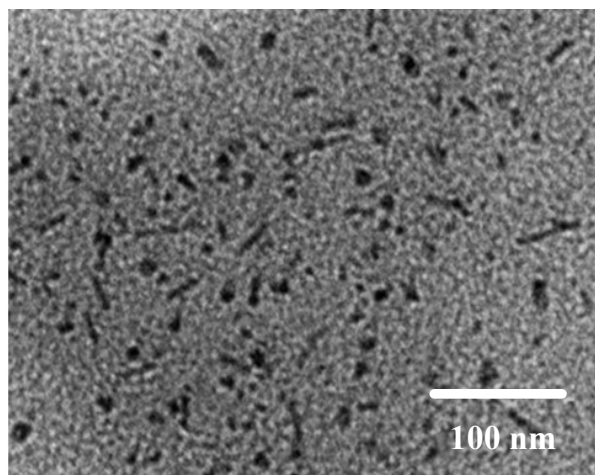


Fig. S15 TEM image of Au(I)-TCEP-Cd(II) after adding DPA (pH 9)

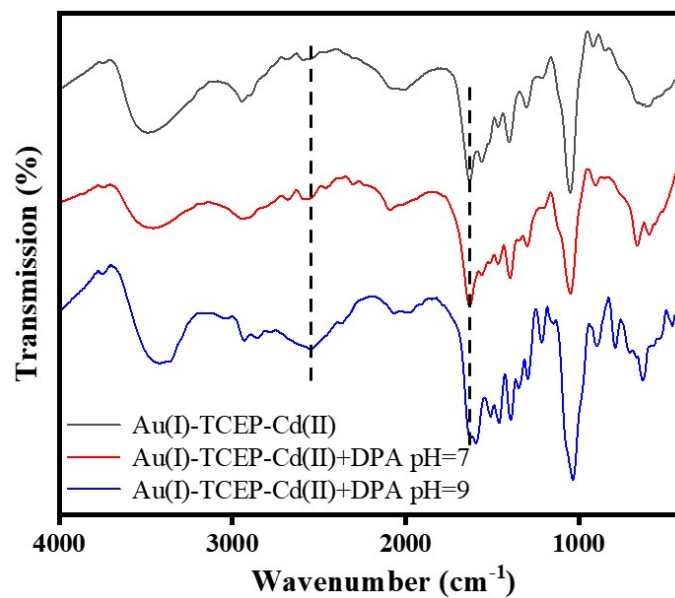


Fig. S16 Comparative FTIR spectra of Au(I)-TCEP-Cd(II) before and after DPA addition (pH 7 and pH 9)

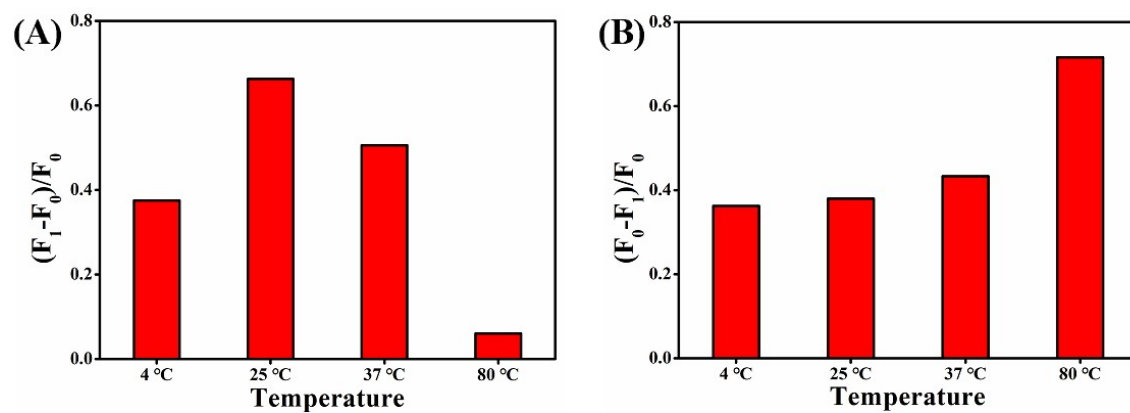


Fig. S17 Detection performance of DPA by Au(I)-TCEP-Cd(II) under different temperatures at pH 7 (A) and pH 9 (B).

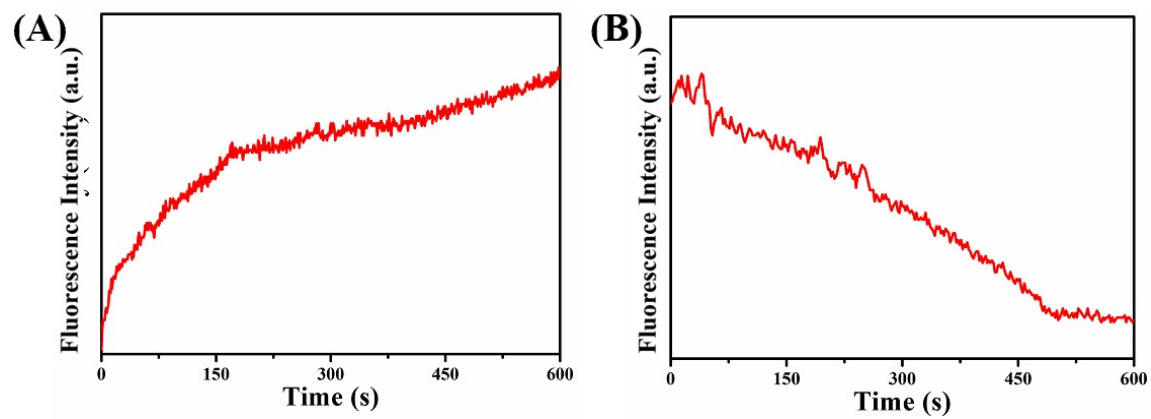


Fig. S18 Detection performance of DPA by Au(I)-TCEP-Cd(II) with different times at pH 7 (A) and pH 9 (B).

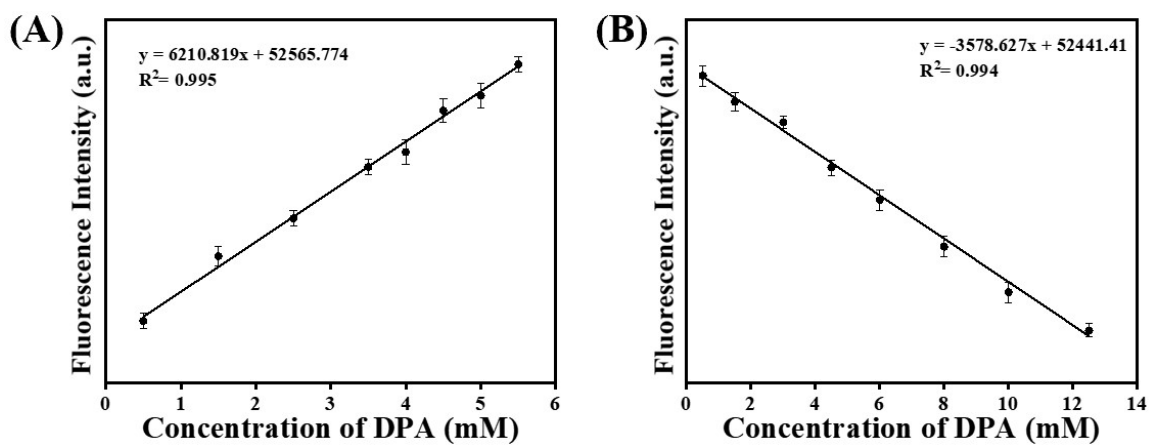


Fig. S19 Fluorescence intensity of Au(I)-TCEP-Cd(II) nanoaggregates as a function of DPA concentration at pH 7 (A) and pH 9 (B).

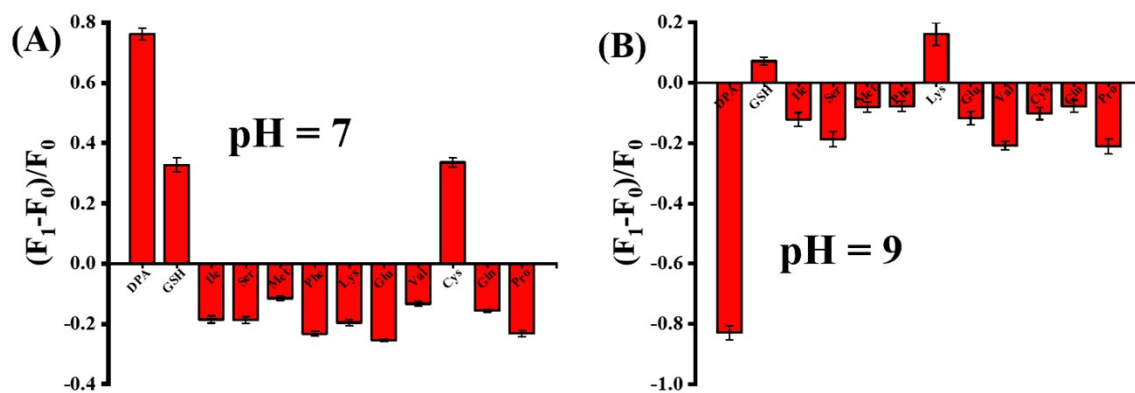


Fig. S20 Selectivity of Au(I)-TCEP-Cd(II) nanoaggregates for various biomolecules at pH 7 (A) and pH 9 (B).

2. Supporting Table

Table S1 Comparison of different methods for the detection of DPA.

Mode	System	Adopted Dual- Mode Verification	Detection Time	Reference
Fluorometry Colorimetry	Cl ⁻ -Cu ²⁺ -OPD	YES	45 min	[31]
Colorimetry	Cu-NC	NO	30 min	[32]
Fluorometry	DNA-AgNCs	NO	20 min	[33]
Ratiometry	N-Ti ₃ C ₂ QDs	YES	3.5 h	[34]
Ratiometry	CDs	YES	3 h	[35]
Ratiometry	Au(I)-TCEP-Cd(II)	YES	8 min	This work

Table S2 Recovery of DPA from serum sample spiked with 2.0 mM DPA

Entry	Serum sample (pH)	Concentration DPA added (mM)	Concentration DPA found (mM)	Recovery %
1	7	2.00	1.89	94.5%
2	7	2.00	1.95	97.5%
3	7	2.00	1.90	95.0%
4	9	2.00	1.85	92.5%
5	9	2.00	1.89	94.5%
6	9	2.00	1.82	91.0%